RNA (1997), 3:702–709. Cambridge University Press. Printed in the USA.

Base dynamics in a UUCG tetraloop RNA hairpin characterized by ^{15}N spin relaxation: Correlations with structure and stability

MIKAEL AKKE,[1] RADOVAN FIALA,[2] FENG JIANG,[2] DINSHAW PATEL,[2] and ARTHUR G. PALMER III[1]

[1]Department of Biochemistry and Molecular Biophysics, Columbia University, New York, New York 10032, USA
[2]Cellular Biochemistry and Biophysics Program, Memorial Sloan-Kettering Cancer Center, New York, New York 10021, USA

ABSTRACT

Intramolecular dynamics of guanine and uracil bases in a 14-nt RNA hairpin including the extraordinarily stable UUCG tetraloop were studied by ^{15}N spin relaxation experiments that are sensitive to structural fluctuations occurring on a time scale of picoseconds to nanoseconds. The relaxation data were interpreted in the framework of the anisotropic model-free formalism, using assumed values for the chemical shift anisotropies of the ^{15}N spins. The rotational diffusion tensor was determined to be symmetric with an axial ratio of 1.34 ± 0.12, in agreement with estimates based on the ratio of the principal moments of the inertia tensor. The model-free results indicate that the bases of the G·U pair in the tetraloop are at least as rigid as the interior base pairs in the stem, whereas the 5′-terminal guanine is more flexible. The observed range of order parameters corresponds to base fluctuations of 19–22° about the χ torsion angle. The results reveal dynamical consequences of the unusual structural features in the UUCG tetraloop and offer insights into the configurational entropy of hairpin formation.

Keywords: anisotropic rotational diffusion; conformational fluctuations; entropy; order parameter

INTRODUCTION

The RNA sequence CUUCGG is an abundant structural element of extraordinarily high stability (Tuerk et al., 1988; Antao et al., 1991; Antao & Tinoco, 1992) that has been proposed to function as a nucleation site for RNA folding and as a protein recognition site (Tuerk et al., 1988; Varani, 1995). The underlined UUCG sequence forms a tetraloop, and the bracketing nucleotides form a closing base pair that occurs with high frequency (Varani, 1995). Solution NMR studies of the UUCG tetraloop have revealed a compact structure that exhibits extensive base stacking and a large number of additional favorable intramolecular interactions. The U·G base pair (with the G in *syn* conformation) between the first and last tetraloop nucleotides involves both base–base and base–sugar hydrogen bonds. A kink in the phosphodiester backbone between the first and second nucleotides (U-U) provides the requisite strand reversal, and is stabilized by hydrogen bonds between a phosphate oxygen and the exocyclic amino group of the C in position three. The second and third nucleotides (U-C) assume unusual torsion angles, including the extended 2′-*endo* ribose conformation; the γ torsion angle of the fourth nucleotide (G) adopts the *trans* conformation (Cheong et al., 1990; Varani et al., 1991; Allain & Varani, 1995). The base of the U in position two appears to be largely disordered, and does not provide any stabilizing interactions (Cheong et al., 1990; Varani et al., 1991; Allain & Varani, 1995). The characteristic structure of the tetraloop, rather than the stability per se (Selinger et al., 1993), prevents reverse transcriptase from reading through the sequence (Tuerk et al., 1988) and imparts resistance against nucleases (Adams & Stern, 1990).

The UNCG and GNRA families of stable RNA hairpins (where N is any nucleotide and R is purine) have very similar overall folds (Cheong et al., 1990; Heus & Pardi, 1991; Varani et al., 1991; Allain & Varani, 1995). However, the biological roles of these two sequences appear different. GNRA loops often are involved in tertiary interactions in larger RNAs and also function as protein binding sites, whereas UNCG loops have not been observed yet in tertiary RNA contacts, and are implied less frequently in protein recognition (Va-

Reprint requests to: Arthur G. Palmer III, Department of Biochemistry and Molecular Biophysics, Columbia University, 630 West 168th Street, New York, New York 10032, USA; e-mail: agp6@columbia.edu.

rani, 1995). These differences have been attributed to distinct dynamical properties of the two sequences: the GNRA family appears more flexible and tolerant of conformational changes important for molecular recognition (Varani, 1995). In keeping with this hypothesis, UNCG tetraloops are more stable than GNRA tetraloops (Antao et al., 1991; Antao & Tinoco, 1992). The thermodynamics of UUCG tetraloop formation involve negative values of both ΔH and ΔS that are roughly twice as large as those for moderately stable tetraloops, e.g., UUUU (Antao & Tinoco, 1992). Furthermore, estimates based on nearest-neighbor effects (Freier et al., 1986) suggest that ΔH and ΔS of UUCG tetraloop formation are of larger magnitude than the values expected for the same sequence forming a terminal mismatched duplex.

In order to delineate the relationships between the structures, thermodynamic stabilities, and biological functions of tetraloops, structural studies must be complemented by characterization of equilibrium conformational fluctuations. Measurement of nuclear spin relaxation by NMR spectroscopy is a powerful approach for studying conformational fluctuations at atomic resolution (Kowalewski, 1989, 1991). A number of methods have been developed to interpret spin relaxation data in terms of intramolecular dynamic processes (London, 1980; Heatley, 1986). Currently, the most common treatments for globular macromolecules are the model-free formalism (Lipari & Szabo, 1982) and the spectral density mapping procedure (Peng & Wagner, 1992; Farrow et al., 1995; Ishima & Nagayama, 1995). The former parameterizes the amplitudes and time scales of intramolecular motions with minimal specification of a particular motional model. The latter evaluates the spectral density function directly at certain discrete frequencies. The amplitudes of the bond vector reorientations provide an estimate of the configurational entropic contribution to molecular processes, such as folding and ligand binding (Akke et al., 1993; Yang & Kay, 1996). Previous spin relaxation studies of nucleic acid dynamics generally can be divided into two categories that depend on the size and shape of the molecules. Large DNA duplexes have highly anisotropic geometries and undergo collective bending and twisting motions of the helix that require the molecules to be modeled as flexible rods, reviewed in Robinson and Drobny (1995). In contrast, shorter duplexes and hairpins are compact molecules for which overall and internal motions are essentially decoupled; consequently, the intramolecular dynamics can be analyzed successfully using the model-free approach (Williamson & Boxer, 1989; Borer et al., 1994; King et al., 1995) or simple physical models (Wang et al., 1994; Gaudin et al., 1995).

The recent development of techniques for the preparation of RNA molecules uniformly enriched with ^{15}N and ^{13}C spin-1/2 stable isotopes (Batey et al., 1992, 1995; Nikonowicz et al., 1992; Varani et al., 1996) have made possible the study of RNA by multidimensional heteronuclear NMR methods (Nikonowicz & Pardi, 1993; Pardi, 1995; Varani et al., 1996). In addition to simplifying structure determination, isotopic labeling makes possible the characterization of intramolecular dynamics by heteronuclear spin relaxation experiments (King et al., 1995).

The 14-nt hairpin GGCACUUCGGUGCC (Fig. 1) forms an integral part of a 40-nt ATP-binding aptamer, the structure of which was determined recently in solution by NMR methods (Jiang et al., 1996). As an initial stage in characterizing the role of conformational dynamics in structure, stability, and function of RNA motifs, the internal dynamics of guanine and uracil bases in the 14-nt hairpin have been characterized on a picosecond to nanosecond time scale using ^{15}N spin relaxation NMR spectroscopy. The paucity of information on the chemical shift anisotropies of base imino ^{15}N spins renders the absolute quantifications of structural fluctuations uncertain, but useful information on the relative motional amplitudes of individual nucleotide bases is obtained. The results provide insights into entropic contributions from changes in conformational fluctuations to the process of hairpin formation, and form the basis for further studies on the sequence- and context-dependent dynamics of RNA motifs.

RESULTS AND DISCUSSION

The 14-nt hairpin contains five guanines and three uracils. Spin-lattice (R_1) and spin-spin (R_2) relaxation rate constants and $\{^1H\}$-^{15}N NOEs were obtained for seven of these nucleotides. Data were not obtained for U7 (in position two of the loop), which has few interactions with the rest of the nucleotides, and whose imino proton is in fast exchange with solvent protons. The relaxation parameters are presented in Table 1. Parameter values range from 1.90–2.20 (mean = 2.04 ± 0.11) s^{-1} for R_1, 5.70–6.40 (mean = 6.19 ± 0.23) s^{-1} for R_2, and 0.71–0.75 (mean = 0.74 ± 0.01) for the NOE.

Rotational diffusion anisotropy

The diffusion tensor was calculated using Equation 5. The F statistic comparing analyses including and excluding G1 indicates that exclusion of G1 improves the

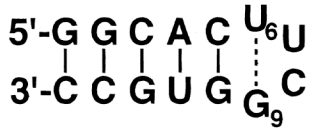

FIGURE 1. Diagram of the 14-nt hairpin. Base pairs in the stem are indicated by solid vertical lines. The mismatched base pair between U6 and G9 in the tetraloop is indicated by a dashed vertical line.

TABLE 1. Model-free and relaxation parameters.

Residue	S^2	τ_e (ps)	θ (°)	R_1 (s^{-1})	R_2 (s^{-1})	NOE
G1[a]	0.74 ± 0.01	—	—	1.95 ± 0.06	6.24 ± 0.14	0.74 ± 0.02
G2	0.787 ± 0.003	—	56 ± 8	2.09 ± 0.02	6.40 ± 0.03	0.750 ± 0.006
U6	0.773 ± 0.008	9 ± 4	38 ± 13	1.94 ± 0.03	6.21 ± 0.08	0.71 ± 0.01
G9	0.807 ± 0.002	4 ± 2	79 ± 5	2.20 ± 0.01	6.37 ± 0.02	0.733 ± 0.004
G10	0.776 ± 0.003	—	80 ± 9	2.10 ± 0.01	6.13 ± 0.03	0.741 ± 0.005
U11	0.760 ± 0.004	—	79 ± 5	1.97 ± 0.02	5.70 ± 0.03	0.741 ± 0.005
G12	0.780 ± 0.003	—	63 ± 6	2.12 ± 0.02	6.26 ± 0.03	0.750 ± 0.006

[a]G1 was optimized with an isotropic model using S^2 and a value for τ_c = 5.7 ± 0.2. This corresponds to a calculated effective θ = 31°, as discussed in the text.

rotational diffusion analysis (at the 90% confidence level; p = 0.089). The local diffusion coefficient, D, for G1 deviates from Equation 6, whereas the values of D for the other bases adhere to the equation (data not shown). Because G1 is the 5′-terminal base, the N-H bond vector may sample a wide range of orientations due to fraying of the duplex, and the orientation of the bond vector in the molecular model may not be accurate. Accordingly, G1 was excluded from the final analysis to yield the ratio $D_\parallel/D_\perp$ = 1.34 ± 0.12 and the effective overall rotational correlation time $\tau_c = (6D_{iso})^{-1}$ = 5.4 ± 0.1 ns [corresponding to $D_\perp$ = (2.77 ± 0.11)·10^7 s^{-1} and $D_\parallel$ = (3.71 ± 0.21)·10^7 s^{-1}]. Jackknife analyses (Mosteller & Tukey, 1977) indicated that the reported uncertainties may be overestimated by 40–50%. F-statistical testing indicates that the axially symmetric model is a significant improvement over the isotropic model (p = 0.010), whereas the fully anisotropic model is not significantly better than the axially symmetric model. The axially symmetric model and the value of $D_\parallel/D_\perp$ obtained here are in reasonable agreement with estimates based on the principal moments of the inertia tensor. Discounting the effects of hydration, which tend to reduce the apparent rotational anisotropy, the relative values of 1.00, 0.97, 0.42, yield $I_\parallel/I_\perp$ = 0.43 and correspond to $D_\parallel/D_\perp$ = 1.54. As noted below, the anisotropic distribution of N-H bond vector orientations over the sphere in the RNA hairpin and paucity of data results in relatively poor precision for the principal components of the diffusion tensor.

Model-free analysis

Model-free parameters are summarized in Table 1, and the order parameters are coded onto the structure in Figure 2. Using the axially symmetric diffusion tensor determined above, the relaxation data for six bases were represented adequately by simple models for the spectral density function. G2, G10, U11, and G12 were optimized using S^2 only. U6 and G9 were optimized using S^2 and τ_e. The generalized order parameter for G1 was optimized using the isotropic diffusion model and $\tau_c = (6D)^{-1}$ = 5.7 ns derived from R_2/R_1. Using the global values of $D_\perp$ and $D_\parallel$, this value of D implies an effective polar angle $\theta \approx 35°$, compared to $\theta \approx 51°$ for G1 in the hairpin model. The values of S^2 vary

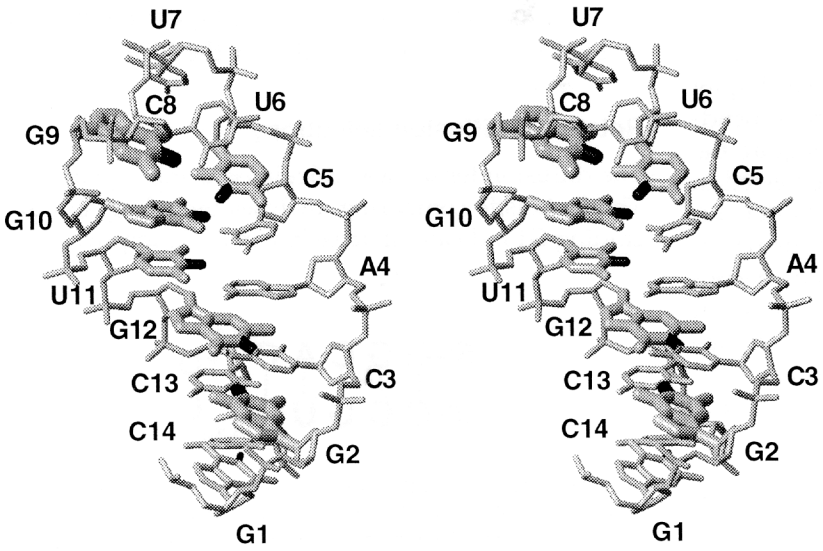

FIGURE 2. Stereo view of the hairpin model. The order parameters are coded onto the bases using a continuous scale of bond thickness, with S^2 = 0.74 (thin) for G1 to S^2 = 0.81 (thickest) for G9. The N-H bond vectors of the characterized spins are highlighted in black. The backbone and ribose moieties, as well as the noncharacterized bases (U7 and the adenine and cytosine bases) are depicted using thinner bonds. For clarity, only heavy atoms are shown (except for protons attached directly to the characterized nitrogen atoms), and oxygens of the ribose rings are omitted. The figure was prepared using MOLMOL (Koradi et al., 1996), generously made available by the laboratory of Professor K. Wüthrich.

between 0.74 and 0.81. The lowest value is obtained for G1 and the highest value is obtained for G9, the critical fourth nucleotide of the tetraloop. U6, which forms a base pair with G9, has a value of S^2 of 0.77, similar to the values for bases in the stem (G2, G10, U11, G12), which range between 0.76–0.79. As mentioned above, the ambiguity in the values of the ^{15}N CSA in the imino groups obfuscates comparisons between order parameters for U and G nucleotides. The order parameters obtained here agree with those reported previously for nucleotide base C-H bond vectors in short DNA duplexes, $S^2 \sim 0.7$–0.8 (Borer et al., 1994), and in the stem and terminal loop of a 29-nt segment of the HIV-1 ΔTAR RNA, $S^2 \sim 0.6$–0.9 (King et al., 1995), but are significantly larger than those observed in a DNA pentaloop, $S^2 \sim 0.5$–0.65 (Williamson & Boxer, 1989). Bases in the stem do not require an effective correlation time constant for the internal motion, τ_e, in the model-free optimization, whereas U6 and G9 do, suggesting that the time scale of base dynamics are different for the G·U pair in the tetraloop and the stem base pairs. A similar pattern was observed in ΔTAR RNA, where bases in the bulge and loop had significantly higher internal correlation times than those in the stem (King et al., 1995). More detailed interpretation of τ_e requires specification of a motional model (Lipari & Szabo, 1982) and is not attempted herein.

Base plane fluctuations

The mean value and standard deviation of the angle β between the N-H bond vector and the $C_{1'}$-N glycosidic bond vector, as calculated for the hairpin model, were $59.0 \pm 1.8°$ and $70.68 \pm 0.03°$ for guanine and uracil, respectively. Using these mean values, the range of order parameters correspond to base plane fluctuations around the χ torsion angle of $\sigma_\chi = 19$–$22°$, as obtained from Equation 7. These values should be taken as upper bounds on the base plane fluctuations, because the effects of possible librational motions of the N-H bond vector in the frame of the base plane have not been considered prior to application of Equation 7; σ_χ may be decreased by ~4° if fast librations reduce the time correlation function to 0.90–0.95, as is typically seen in molecular dynamics simulations (Palmer & Case, 1992). The values of σ_χ agree with previous evaluations of χ torsion angle fluctuations in nucleotides. In a solid-state ^2H NMR study of purine motion in a 12-base pair RNA duplex, the experimental data were described best by the "restricted diffusion on a cone" model (Wittebort & Szabo, 1978), using an amplitude of angular excursions $\Delta\chi$ of $19 \pm 12°$ (Wang et al., 1994). Thymine $^{13}C_{1'}$ relaxation in a DNA dodecamer in solution has been modeled by restricted rotation around the $C_{1'}$-N_1 bond with $\Delta\chi = 28°$ (Gaudin et al., 1995). The χ torsion angle is one of the major determinants of nucleic acid structure (Saenger, 1984); consequently, characterization of fluctuations around this torsion angle is of particular relevance for improving atomic descriptions of nucleic acid structural dynamics.

Correlations between structure, stability, and dynamics

The present results provide information on the relative amplitude of internal motions on a time scale of picoseconds to nanoseconds. The most significant results concern the base pair in the tetraloop: G9 is the least flexible base in the entire hairpin and U6 is approximately as rigid as bases in the stem. These observations complement the results from previous studies on stability and structure of the UUCG tetraloop (Cheong et al., 1990; Antao et al., 1991; Varani et al., 1991; Antao & Tinoco, 1992; Allain & Varani, 1995). As discussed above, UUCG tetraloop formation involves favorable enthalpy and unfavorable entropy of unusually large magnitudes. The structural basis for the favorable enthalpy of tetraloop formation is revealed by the recent high-resolution NMR structure, which showed that the U6 and G9 bases form a unique base pair, and are well stacked onto the stem of the hairpin structure (Allain & Varani, 1995). The base of G9 forms three hydrogen bonds involving both the base and ribose moieties of U6: the exocyclic amino group as well as N_1-H_1 of G9 interact with O_2 of U6, whereas O_6 of G9 interacts with the 2′-hydroxyl group of U6; N_3-H_3 of U6 is not involved in any hydrogen bonds. Comparisons of the order parameters of G9, on the one hand, and the mean of the internal stem guanines (G2, G10, G12), on the other, yield insights into the molecular basis for the thermodynamic stability of the UUCG tetraloop. A higher degree of motional restriction may be a signature of more favorable interaction enthalpy. Thus, the present results are in consonance with the thermodynamic and structural data: the base of G9 is slightly more restrained motionally than the corresponding bases in the stem. Order parameters can be used to estimate an upper bound on the change in free energy and entropy (Akke et al., 1993; Yang & Kay, 1996) that result from motional restriction. The small differences in S^2 values between G9 and the stem guanines, and between U6 and U11, indicate that the entropic penalty associated with tetraloop formation arising from changes in fluctuations of these nucleotide bases is comparable to that of duplex formation. In contrast, the ribose rings of the second and third nucleotides in the tetraloop populate exclusively the $C_{2'}$-*endo* conformer (Cheong et al., 1990; Varani et al., 1991), and therefore appear to be quite rigid. Taken together, these data may suggest that the unfavorable entropy of forming the UUCG tetraloop involves larger contributions from motional restriction of the backbone than

the bases, relative to a duplex. Complementary data on ^{13}C (Borer et al., 1994; King et al., 1995) and ^{31}P (Schweitzer et al., 1995) spin relaxation in the ribose moieties and phosphate backbone, respectively, will be useful for further characterization of the backbone fluctuations.

MATERIALS AND METHODS

Theory

Relaxation of an imino ^{15}N spin is dominated by the dipolar interaction with the directly attached ^1H spin and by the chemical shift anisotropy (CSA). The spin-lattice, spin-spin, and steady-state NOE relaxation parameters are given by (Abragam, 1961):

$$R_1 = (d^2/4)[J(\omega_H - \omega_N) + 3J(\omega_N) + 6J(\omega_H + \omega_N)] + c^2J(\omega_N), \quad (1)$$

$$R_2 = (d^2/8)[4J(0) + J(\omega_H - \omega_N) + 3J(\omega_N) + 6J(\omega_H) + 6J(\omega_H + \omega_N)] + (c^2/6)[4J(0) + 3J(\omega_N)] + R_{ex}, \quad (2)$$

$$\mathrm{NOE} = 1 + (d^2/4R_1)(\gamma_N/\gamma_H) \times [6J(\omega_H + \omega_N) - J(\omega_H - \omega_N)], \quad (3)$$

respectively, in which $d = \mu_0 h\gamma_N\gamma_H\langle r_{NH}^{-3}\rangle/8\pi^2$; $c = \omega_N\Delta\sigma/\sqrt{3}$; μ_0 is the permeability of free space; h is Planck's constant; γ_H and γ_N are the gyromagnetic ratios of ^1H and ^{15}N, respectively; $r_{NH} = 1.01$ Å is the nitrogen-hydrogen bond length, chosen slightly larger than the vibrationally averaged values obtained using the AMBER or CHARMM potentials (Cornell et al., 1995; MacKerell et al., 1995); ω_H and ω_N are the Larmor frequencies of ^1H and ^{15}N, respectively; R_{ex} is a parameter that accounts for possible contributions from conformational exchange to the transverse relaxation rate (Bloom et al., 1965); and $\Delta\sigma$ is the CSA, assumed to have values of -130 and -100 ppm for guanine N_1 spins and uracil N_3 spins, respectively (see below). The dipolar interaction strengths for ^{13}C-^{15}N and ^1H-^{15}N spin pairs have the ratio $d_{NC}^2/d_{NH}^2 = \gamma_C^2\langle r_{NH}^{-6}\rangle/(\gamma_H^2\langle r_{NH}^{-6}\rangle) \approx 1\%$; thus, the presence of ^{13}C nuclei in the doubly labeled sample does not impact significantly on the relaxation measurements. The amplitudes and time scales of the intramolecular motions are determined from the relaxation data by using the model-free formalism (Lipari & Szabo, 1982; Clore et al., 1990). In the present case, the spectral density function accounts for axially symmetric overall rotational diffusion and independent internal motions of the N-H bond vector in the principal axis frame of the diffusion tensor (Halle & Wennerström, 1981; Lipari & Szabo, 1982; Schurr et al., 1994; Zheng et al., 1995):

$$J(\omega) = \frac{2}{5}\left\{S^2\left[\sum_{k=0}^{2}\frac{A_k\tau_k}{1 + (\omega\tau_k)^2}\right] + (1 - S^2)\left[\sum_{k=0}^{2}\frac{A_k\tilde{\tau}_k}{1 + (\omega\tilde{\tau}_k)^2}\right]\right\}, \quad (4)$$

in which $\tau_k^{-1} = 6D_\perp - k^2(D_\perp - D_\parallel)$, $\tilde{\tau}_k = \tau_e\tau_k/(\tau_e + \tau_k)$; $D_\parallel$ and $D_\perp$ are principal components of the diffusion tensor parallel and perpendicular, respectively, to the unique axis; τ_e is the effective correlation time for internal motions on a fast time scale defined by $(\omega_H - \omega_N)^2\tau_e^2 \ll 1$; $A_0 = (1/4) \times (3\cos^2\theta - 1)^2$; $A_1 = 3\sin^2\theta\cos^2\theta$; $A_2 = (3/4)\sin^4\theta$; θ is the angle between the N-H bond vector and the unique axis of the diffusion tensor; and S^2 is the square of the generalized order parameter characterizing the amplitude of the internal motion. Generalized order parameters range from zero for isotropic internal motions to unity for completely restricted motion in a molecular reference frame. In the following, S^2 is referred to simply as the "order parameter."

The degree of rotational diffusion anisotropy can be determined from the R_2/R_1 ratios (Tjandra et al., 1995; Zheng et al., 1995) or local diffusion constants D (Brüschweiler et al., 1995; Lee et al., 1997) for each spin; the latter approach was used in the present study. Briefly, a set $\{D\}$ is obtained by fitting an isotropic diffusion model to the R_2/R_1 ratios for those bond vectors that experience only fast internal motions of low amplitude (i.e., τ_e and $1 - S^2$ are small). For low degrees of anisotropy of an axially symmetric tensor (Brüschweiler et al., 1995; Lee et al., 1997):

$$D = (D_\perp + D_\parallel)/2 + (D_\perp - D_\parallel)(a_{31}x + a_{32}y + a_{33}z)^2/2, \quad (5)$$

in which $\mathbf{e} = (x, y, z)$ are the direction cosines of the N-H bond vector in a molecular frame, as obtained from a model structure of the RNA hairpin (see below); and $a_{31} = \sin\theta_D\cos\phi_D$, $a_{32} = \sin\theta_D\sin\phi_D$, and $a_{33} = \cos\theta_D$ define the orientation of the symmetry axis of the diffusion tensor in the molecular frame. In the principal axis frame of the diffusion tensor, Equation 5 reduces to:

$$D = D_{iso} - (3\cos^2\theta - 1)(D_\parallel - D_\perp)/6, \quad (6)$$

in which $D_{iso} = 2(D_\perp + D_\parallel)/3$. Equation 6 provides a convenient way of evaluating the distribution of bond vector orientations in the diffusion frame. Expressions for isotropic and anisotropic diffusion have been given elsewhere (Brüschweiler et al., 1995; Lee et al., 1997).

Order parameters can be interpreted in terms of specific motional models. A particularly useful interpretation of the order parameters in the present system is given by the Gaussian axial fluctuation (GAF) model (Brüschweiler & Wright, 1994), which describes a Gaussian distribution of bond vector orientations on the surface of a cone:

$$S^2 = 1 - 3\sin^2\beta\{\cos^2\beta(1 - \exp[-\sigma_\chi^2]) + (1/4)\sin^2\beta(1 - \exp[-4\sigma_\chi^2])\} \quad (7)$$

in which β is the (fixed) angle between the bond vector equilibrium position and the director axis for the motion (the axis of the cone), and σ_χ is the standard deviation of the fluctuation in the azimuthal angle. The GAF model is a modification of the "restricted diffusion on a cone" model (Wittebort & Szabo, 1978) to include a harmonic potential.

In order to use the GAF model to relate the order parameter of the imino nitrogens to fluctuations of the plane of the pyrimidine or purine heterocycle, β is defined as the angle between the imino ^{15}N-^{1}H bond vector and the $C_{1'}$-N glycosidic bond vector, and σ_χ is defined as the standard deviation of the χ torsion angle fluctuation. The angle β varies slightly with glycosidic conformation (Saenger, 1984).

The magnitudes of the principal components of the ^{15}N chemical shift tensor and the orientation of the tensor axes with respect to ^{15}N-^{1}H bond vector are of importance for the relaxation of the ^{15}N spin. The chemical shift tensors for the imino ^{15}N spins in RNA molecules are not known. However, the ^{15}N chemical shift tensors have been determined for nonglycosylated uracil by solid-state NMR methods and ab initio calculations (Anderson-Altmann et al., 1995). The experimental results indicate that the N_3 shift tensor is asymmetric (nonaxial) with $\Delta\sigma = -95$ ppm and an asymmetry parameter of $\eta = 0.82$. The least shielded component is oriented at an angle of 9° from the N-H bond vector. Furthermore, the ab initio calculations indicate that hydrogen bonding increases the asymmetry (Anderson-Altmann et al., 1995). In the sample used in the solid-state NMR study, the uracil N_3-H_3 imino group is hydrogen bonded to a carbonyl oxygen of a neighboring molecule, whereas in RNA duplexes, the hydrogen bonding partner of the imino group is a nitrogen atom (Saenger, 1984). Because N-H-N hydrogen bonds are expected to be weaker than N-H-O bonds (Jeffrey & Saenger, 1991), the asymmetry may be smaller in RNA than in free uracil. In the present study, relaxation data were interpreted under the assumptions that the chemical shift tensors for N_1 in G and N_3 in U are axially symmetric and coaxial with the N-H bond vectors. A value of $\Delta\sigma = -100$ ppm was calculated from the principal components of the shift tensor (Anderson-Altmann et al., 1995). Preliminary studies, using cross-correlation relaxation experiments (Tjandra et al., 1996), indicate that the absolute value of $\Delta\sigma$ for guanine N_1 spins is roughly 30 ppm larger than for uracil N_3 spins (M. Akke & R. Fiala, unpubl.); consequently, a value of $\Delta\sigma = -130$ ppm was used for guanine N_1. The CSA mechanism is estimated to contribute ~8% and ~12% of the total relaxation of U and G, respectively, at a static magnetic field strength of 11.7 T. The error associated with neglecting the asymmetry of the shift tensor is estimated to be less than 2% and 3% for U and G, respectively, over the range $\eta = 0$–0.82 and $\sigma_\chi < 30°$, as gauged from calculations employing the GAF model (Brüschweiler & Wright, 1994) implemented for an anisotropic shift tensor and isotropic overall rotational diffusion (Denisov & Halle, 1995). Because the CSA appears to be different for G and U, and the actual values are not known precisely, comparisons of order parameters for different types of nucleotides should be made with caution. Also, variations in the magnitude of $\Delta\sigma$ arising from variations in local chemical environment translate into slight differences, ΔS^2, in the values of S^2 (Tjandra et al., 1996). Numerical simulations indicate that $\Delta S^2 = [0.0015\cdot(\Delta\sigma + 100)]S^2$ over the ranges $S^2 = 0.6$–0.9 and $\Delta\sigma = -120$ to -80 ppm, in which S^2 is the order parameter obtained using $\Delta\sigma = -100$ ppm. For a 20% variation in $\Delta\sigma$, $\Delta S^2/S^2 \leq 3\%$. Thus, the relative error in comparisons of order parameters for nucleotides of the same type is not affected critically by inaccuracies in the value of $\Delta\sigma$.

Sample preparation

The 14-nt hairpin GGCACUUCGGUGCC was synthesized by in vitro transcription from a DNA template with (^{13}C, ^{15}N)-labeled nucleoside triphosphates using T7 RNA polymerase and purified by gel electrophoresis (Batey et al., 1992; Nikonowicz et al., 1992). The final sample concentration was 4 mM RNA, 10 mM sodium phosphate, and 0.2 mM EDTA, dissolved 90% H_2O/10% D_2O at pH 6.7.

NMR spectroscopy

All NMR experiments were recorded on a Varian Unity Plus 500 spectrometer at a temperature of 273.0 ± 0.1 K. R_1, R_2, and NOE for the imino ^{15}N nuclei were measured by two-dimensional sensitivity-enhanced proton-detected heteronuclear NMR spectroscopy, using pulse sequences described previously (Farrow et al., 1994). The R_1 and R_2 experiments utilized relaxation delays of 68.9, 143.1 (×2), 233.2, 344.5, 487.6, 694.3, 1,038.8 (×2), 1,499.9 ms, and 33.7, 71.8 (×2), 115.8, 167.9, 231.7, 313.9, 429.7 (×2), 627.8 ms, respectively (×2 indicates duplicate experiments). The NOE was measured from pairs of spectra recorded with and without proton saturation during the recycle delay. Proton saturation during the NOE experiment was achieved by applying a GARP-1 pulse train (Shaka et al., 1985), centered in the imino region, with a field strength of 805 Hz for 5 s. The control experiment without proton saturation used a recycle delay of 6.5 s, with continuous wave ^{1}H irradiation of 805 Hz field strength, applied 200 ppm off resonance for the last 5 s. In all experiments, the spectral widths were 2,000 Hz sampled over 64 complex points and 12,500 Hz sampled over 4,096 complex points in the ^{15}N and ^{1}H dimensions, respectively. The spectra were processed by applying a convolution difference filter to suppress the residual solvent signal (Marion et al., 1989), followed by a cosine bell apodization function and zero-filling once in the acquisition dimension; a Kaiser apodization function over all 128 points followed by zero-filling to 512 points were applied in the indirect dimension. A fifth-order polynomial baseline correction was applied in the acquisition dimension. Processing of spectra and evaluation of peak intensities were performed using Felix 2.3 (MSI).

Data analysis

Relaxation parameters were determined from the peak heights and uncertainties by nonlinear optimization using the Levenberg–Marquardt algorithm (Press et al., 1986), as described (Palmer et al., 1991). Peak height uncertainties were determined from duplicate spectra for the R_1 and R_2 experiments (Palmer et al., 1991; Skelton et al., 1993). Uncertainties in parameter estimates were obtained from the covariance matrices (Press et al., 1986), or using the jackknife procedure (Mosteller & Tukey, 1977). The standard deviation of the baseplane noise was used to determine the peak height uncertainties for the NOE experiments. Uncertainties in the NOE values were calculated by propagating the uncertainties in the peak heights. The principal components, $D_\parallel$ and $D_\perp$, and the orientation of the diffusion tensor in the molecular frame are obtained by simultaneous optimization of Equation 5 against all data pairs D and $\mathbf{e}$. The determination of the diffusion tensor is hindered somewhat because the dis-

tribution of imino N-H bond vector orientations in the RNA stem is centered in a plane roughly orthogonal to the stem axis (Mackay et al., 1996; Lee et al., 1997), and because the paucity of ^1H-^{15}N spin systems in nucleotides offers few data points for optimization. *F*-statistical testing was used to evaluate the significance of the isotropic, axially symmetric and anisotropic diffusion models. The NMR relaxation data were interpreted within the model-free formalism (Lipari & Szabo, 1982), using a version of the program Modelfree (Palmer et al., 1991) that optimizes Equation 4 given the fixed parameters, $D_{\parallel}$, $D_{\perp}$, and θ, as obtained from the rotational diffusion analyses. Selection of models for internal motions were performed using *F*-statistical testing as described (Mandel et al., 1995). Statistical properties of the model-free parameters were obtained as follows: 100 synthetic sets of $D_{\parallel}$, $D_{\perp}$, and θ were calculated from a corresponding set of randomly distributed values of D. For each simulated set of $D_{\parallel}$, $D_{\perp}$, and θ, model-free parameters were determined and uncertainties were calculated from a set of 300 randomly distributed relaxation values (Press et al., 1986; Palmer et al., 1991). The sample deviations of the model-free parameters were taken as the weighted uncertainties of the 100 synthetic data sets.

Molecular modeling

The coordinates of the hairpin ACUUCGGU were obtained from the high-resolution NMR structure 1hlx (Allain & Varani, 1995) of the Protein Data Bank (Bernstein et al., 1977). The additional three base pairs (5′-G-G-C, G-C-C-3′) of the stem extension were built as a regular A-form duplex, linked to the hairpin, and energy minimized while keeping the coordinates of the eight nucleotides from 1hlx fixed, using Discover/InsightII (MSI). The resulting structure is very similar to the corresponding sequence of 1hlx, as expected, with the corresponding bases overlapping closely, and a RMSD for the backbone heavy atoms of 1.47 Å.

ACKNOWLEDGMENTS

We thank Anna Marie Pyle and Dana Abramovitz (Columbia University) for many stimulating discussions, and Lewis E. Kay (University of Toronto) for providing the pulse programs for the relaxation experiments. M.A. gratefully acknowledges a postdoctoral fellowship from the Swedish Natural Sciences Research Council and a travel grant from the Swedish Medical Research Council. This work was supported by NIH grant GM54777 (D.P.), an American Cancer Society Junior Faculty Research Award (A.G.P.), and an Irma T. Hirschl Career Scientist Award (A.G.P.).

Received January 9, 1997; returned for revision February 14, 1997; revised manuscript received April 3, 1997

REFERENCES

Abragam A. 1961. *Principles of nuclear magnetism.* Oxford: Clarendon Press.

Adams CC, Stern DB. 1990. Control of mRNA stability in chloroplasts by 3′ inverted repeats: Effects of stem and loop mutations on degradation of psbA mRNA in vitro. *Nucleic Acids Res 18*:6003–6010.

Akke M, Brüschweiler R, Palmer AG. 1993. NMR order parameters and free energy: An analytical approach and its application to cooperative Ca^{2+} binding by calbindin D_{9k}. *J Am Chem Soc 115*: 9832–9833.

Allain FHT, Varani G. 1995. Structure of the P1 helix from group I self-splicing introns. *J Mol Biol 250*:333–353.

Anderson-Altmann KL, Phung CG, Mavromoustakos S, Zheng Z, Facelli J, Poulter CD, Grant DM. 1995. ^{15}N chemical shift tensors of uracil determined from ^{15}N powder pattern and ^{15}N-^{13}C dipolar NMR spectroscopy. *J Phys Chem 99*:10454–10458.

Antao VP, Lai SY, Tinoco I. 1991. A thermodynamic study of unusually stable RNA and DNA hairpins. *Nucleic Acids Res 19*:5901–5905.

Antao VP, Tinoco I. 1992. Thermodynamic parameters for loop formation in RNA and DNA hairpin loops. *Nucleic Acids Res 20*:819–824.

Batey RT, Battiste JL, Williamson JR. 1995. Preparation of isotopically enriched RNAs for heteronuclear NMR. *Methods Enzymol 261*:300–322.

Batey RT, Inada M, Kujawinski E, Puglisi JD, Williamson JR. 1992. Preparation of isotopically labeled ribonucleotides for multidimensional NMR spectroscopy of RNA. *Nucleic Acids Res 20*:4515–4523.

Bernstein FC, Koetzle TF, Williams GJB, Meyer EF Jr, Brice MD, Rodgers JR, Kennard O, Shimanouchi T, Tasumi M. 1977. The Protein Data Bank: A computer-based archival file for macromolecular structures. *J Mol Biol 112*:535–542.

Bloom M, Reeves LW, Wells EJ. 1965. Spin echos and chemical exchange. *J Chem Phys 42*:1615–1624.

Borer PN, LaPlante SR, Kumar A, Zanatta N, Martin A, Hakkinen A, Levy GC. 1994. ^{13}C-NMR relaxation in three DNA oligonucleotide duplexes: Model-free analysis of internal and overall motion. *Biochemistry 33*:2441–2450.

Brüschweiler R, Liao X, Wright PE. 1995. Long-range motional restrictions in a multidomain zinc-finger protein from anisotropic tumbling. *Science 268*:886–889.

Brüschweiler R, Wright PE. 1994. NMR order parameters of biomolecules: A new analytical representation and application to the Gaussian axial fluctuation model. *J Am Chem Soc 116*:8426–8427.

Cheong C, Varani G, Tinoco I. 1990. Solution structure of an unusually stable RNA hairpin, 5′GGAC(UUCG)GUCC. *Nature 346*:680–682.

Clore GM, Szabo A, Bax A, Kay LE, Driscoll PC, Gronenborn AM. 1990. Deviations from the simple two-parameter model-free approach to the interpretation of nitrogen-15 nuclear magnetic relaxation of proteins. *J Am Chem Soc 112*:4989–4991.

Cornell WD, Cieplak P, Bayly CI, Gould IR, Merz KM, Ferguson DM, Spellmeyer DC, Fox T, Caldwell JW, Kollman PA. 1995. A second generation force field for the simulation of proteins, nucleic acids and organic molecules. *J Am Chem Soc 117*:5179–5197.

Denisov VP, Halle B. 1995. Direct observation of calcium-coordinated water in calbindin D_{9k} by nuclear magnetic relaxation dispersion. *J Am Chem Soc 117*:8456–8465.

Farrow NA, Muhandiram R, Singer AU, Pascal SM, Kay CM, Gish G, Shoelson SE, Pawson T, Forman-Kay JD, Kay LE. 1994. Backbone dynamics of a free and a phosphopeptide-complexed src homology 2 domain studied by ^{15}N NMR relaxation. *Biochemistry 33*:5984–6003.

Farrow NA, Zhang O, Szabo A, Torchia DA, Kay LE. 1995. Spectral density function mapping using ^{15}N relaxation data exclusively. *J Biomol NMR 6*:153–162.

Freier SM, Kierzek R, Jaeger JA, Sugimoto N, Caruthers MH, Neilson T, Turner DH. 1986. Improved free-energy parameters for predictions of RNA duplex stability. *Proc Natl Acad Sci USA 83*:9373–9377.

Gaudin F, Paquet F, Chanteloup L, Beau JM, Nguyen TT, Lancelot G. 1995. Selectively ^{13}C-enriched DNA: Dynamics of the C1′-H1′ vector in $d(CGAAATTTCG)_2$. *J Biomol NMR 5*:49–58.

Halle B, Wennerström H. 1981. Interpretation of magnetic resonance data from water nuclei in heterogeneous systems. *J Chem Phys 75*:1928–1943.

Heatley F. 1986. Nuclear magnetic relaxation and models for backbone motions of macromolecules in solution. *Annu Rep NMR Spectrosc 17*:179–230.

Heus HA, Pardi A. 1991. Structural features that give rise to the unusual stability of RNA hairpins containting GNRA loops. *Science 253*:191–194.

Ishima R, Nagayama K. 1995. Quasi-spectral-density function analysis for nitrogen-15 nuclei in proteins. *J Magn Reson Ser B 108*:73–76.

Jeffrey GA, Saenger W. 1991. *Hydrogen bonding in biological structures*. Berlin: Springer-Verlag.

Jiang F, Kumar RA, Jones RA, Patel DJ. 1996. Structural basis of RNA folding and recognition in an AMP-RNA aptamer complex. *Nature 382*:183–186.

King GC, Harper JW, Xi Z. 1995. Isotope labeling for ^{13}C relaxation measurements on RNA. *Methods Enzymol 261*:436–450.

Koradi R, Billeter M, Wüthrich K. 1996. MOLMOL: A program for display and analysis of macromolecular structures. *J Mol Graphics 14*:51–55.

Kowalewski J. 1989. Nuclear spin relaxation in diamagnetic fluids. Part 1. General aspects and inorganic applications. *Annu Rep NMR Spectrosc 22*:307–414.

Kowalewski J. 1991. Nuclear relaxation in diamagnetic fluids. Part 2. Organic systems and solutions of macromolecules and aggregates. *Annu Rep NMR Spectrosc 23*:289–374.

Lee LK, Rance M, Chazin WJ, Palmer AG. 1997. Rotational diffusion anisotropy of proteins from simultaneous analysis of ^{15}N and $^{13}C^{\alpha}$ nuclear spin relaxation. *J Biomol NMR*. Forthcoming.

Lipari G, Szabo A. 1982. Model-free approach to the interpretation of nuclear magnetic resonance relaxation in macromolecules. I. Theory and range of validity. *J Am Chem Soc 104*:4546–4559.

London RE. 1980. Intramolecular dynamics of proteins and peptides as monitored by nuclear magnetic relaxation measurements. In: Cohen JS, ed. *Magnetic resonance in biology*. New York: Wiley. pp 1–69.

Mackay JP, Shaw GL, King GF. 1996. Backbone dynamics of the c-jun leucine zipper: ^{15}N NMR relaxation studies. *Biochemistry 35*:4867–4877.

MacKerell AD, Wiorkiewicz-Kuczera J, Karplus M. 1995. An all-atom empirical energy function for the simulation of nucleic acids. *J Am Chem Soc 117*:11946–11975.

Mandel AM, Akke M, Palmer AG. 1995. Backbone dynamics of *Escherichia coli* Ribonuclease HI: Correlations with structure and function in an active enzyme. *J Mol Biol 246*:144–163.

Marion D, Ikura M, Bax A. 1989. Improved solvent suppression in one- and two-dimensional NMR spectra by convolution of time-domain data. *J Magn Reson 84*:425–430.

Mosteller F, Tukey JW. 1977. *Data analysis and regression. A second course in statistics*. Reading, Massachusetts: Addison-Wesley.

Nikonowicz EP, Pardi A. 1993. An efficient procedure for assignment of the proton, carbon and nitrogen resonances in $^{13}C/^{15}N$ labeled nucleic acids. *J Mol Biol 232*:1141–1156.

Nikonowicz EP, Sirr A, Legault P, Jucker FM, Baer LM, Pardi A. 1992. Preparation of ^{13}C and ^{15}N labelled RNAs for heteronuclear multi-dimensional NMR studies. *Nucleic Acids Res 20*:4507–4513.

Palmer AG, Case DA. 1992. Molecular dynamics analysis of NMR relaxation in a zinc-finger peptide. *J Am Chem Soc 114*:9059–9067.

Palmer AG, Rance M, Wright PE. 1991. Intramolecular motions of a zinc finger DNA-binding domain from xfin characterized by proton-detected natural abundance ^{13}C heteronuclear NMR spectroscopy. *J Am Chem Soc 113*:4371–4380.

Pardi A. 1995. Multidimensional heteronuclear NMR experiments for structure determination of isotopically labeled RNA. *Methods Enzymol 261*:350–380.

Peng JW, Wagner G. 1992. Mapping spectral density functions using heteronuclear NMR relaxation measurements. *J Magn Reson 98*:308–332.

Press WH, Flannery BP, Teukolsky SA, Vetterling WT. 1986. *Numerical recipes. The art of scientific computing*. Cambridge: Cambridge University Press.

Robinson BH, Drobny GP. 1995. Site-specific dynamics in DNA: Theory. *Annu Rev Biophys Biomol Struct 24*:523–549.

Saenger W. 1984. *Principles of nucleic acid structure*. New York: Springer-Verlag.

Schurr JM, Babcock HP, Fujimoto BS. 1994. A test of the model-free formulas. Effects of anisotropic rotational diffusion and dimerization. *J Magn Reson Ser B 105*:211–224.

Schweitzer BI, Gardner KH, Tucker-Kellogg GT. 1995. HeteroTOCSY-based experiments for measuring heteronuclear relaxation in nucleic acids and proteins. *J Biomol NMR 6*:180–188.

Selinger D, Liao X, Wise JA. 1993. Functional interchangeability of the structurally similar tetranucleotide loops GAAA and UUCG in fission yeast signal recognition particle RNA. *Proc Natl Acad Sci USA 90*:5409–5413.

Shaka AJ, Barker PB, Freeman R. 1985. Computer-optimized decoupling scheme for wideband applications and low-level operation. *J Magn Reson 64*:547–552.

Skelton NJ, Palmer AG, Akke M, Kördel J, Rance M, Chazin WJ. 1993. Practical aspects of two-dimensional proton-detected ^{15}N spin relaxation measurements. *J Magn Reson Ser B 102*:253–264.

Tjandra N, Feller SE, Pastor RW, Bax A. 1995. Rotational diffusion anisotropy of human ubiquitin from ^{15}N NMR relaxation. *J Am Chem Soc 117*:12562–12566.

Tjandra N, Szabo A, Bax A. 1996. Protein backbone dynamics and ^{15}N chemical shift anisotropy from quantitative measurement of relaxation interference effects. *J Am Chem Soc 118*:6986–6991.

Tuerk C, Gauss P, Thermes C, Groebe DR, Gayle M, Guild N, Stormo G, d'Aubenton-Carafa Y, Uhlenbeck OC, Tinoco I, Brody EN, Gold L. 1988. CUUCGG hairpins: Extraordinarily stable RNA secondary structures associated with various biochemical processes. *Proc Natl Acad Sci USA 85*:1364–1368.

Varani G. 1995. Exceptionally stable nucleic acid hairpins. *Annu Rev Biophys Biomol Struct 24*:379–404.

Varani G, Aboul-ela F, Allain FHT. 1996. NMR investigation of RNA structure. *Prog NMR Spectrosc 29*:51–127.

Varani G, Cheong C, Tinoco I. 1991. Structure of an unusually stable RNA hairpin. *Biochemistry 30*:3280–3289.

Wang AC, Kennedy MA, Reid BR, Drobny GP. 1994. A solid-state ^{2}H NMR investigation of purine motion in a 12 base pair RNA duplex. *J Magn Reson Ser B 105*:1–10.

Williamson JR, Boxer SG. 1989. Multinuclear NMR studies of DNA hairpins. 1. Structure and dynamics of d(CGCGTTGTTCGCG). *Biochemistry 28*:2819–2831.

Wittebort RJ, Szabo A. 1978. Theory of NMR relaxation in macromolecules: Restricted diffusion and jump models for multiple internal rotations in amino acid side chains. *J Chem Phys 69*:1722–1736.

Yang D, Kay LE. 1996. Contributions to conformational entropy arising from bond vector fluctuations measured from NMR-derived order parameters: Application to protein folding. *J Mol Biol 263*:369–382.

Zheng Z, Czaplicki J, Jardetzky O. 1995. Backbone dynamics of *trp* repressor studied by ^{15}N NMR relaxation. *Biochemistry 34*:5212–5223.